Rate Constant and Branching Ratio for the Reactions of the Ethyl Peroxy Radical with Itself and with the Ethoxy Radical

Mirna Shamas, Mohamed Assali, Cuihong Zhang, Xiaofeng Tang, Weijun Zhang, Laure Pillier, Coralie Schoemaecker, Christa Fittschen

Rate Constant and Branching Ratio for the Reactions of Ethyl Peroxy Radical with Itself and with Ethoxy Radical

Mirna Shamas[1], Mohamed Assali[1], Cuihong Zhang[1,2], Xiaofeng Tang[2], Weijun Zhang[2], Laure Pillier[1], Coralie Schoemaecker[1] and Christa Fittschen[1,*]

[1] Université Lille, CNRS, UMR 8522 - PC2A - Physicochimie des Processus de Combustion et de l'Atmosphère, F-59000 Lille, France

[2] Laboratory of Atmospheric Physico-Chemistry, Anhui Institute of Optics and Fine Mechanics, HFIPS, Chinese Academy of Sciences, Hefei 230031, Anhui, China

*Corresponding author: Christa Fittschen (christa.fittschen@univ-lille.fr)

Submitted to

Earth and Space Chemistry

ABSTRACT

The self-reaction of the ethyl peroxy radical ($C_2H_5O_2$) (R1) has been studied using laser photolysis coupled to a selective time resolved detection of two different radicals by continuous wave cavity ring-down spectroscopy (cw-CRDS) in the near-infrared range: $C_2H_5O_2$ was detected in the $\tilde{A}$-$\tilde{X}$ electronic transition at 7596 cm^{-1}, and HO_2 was detected in the $2\nu_1$ vibrational overtone transition at 6638.21 cm^{-1}. Radicals were generated from pulsed 351 nm photolysis of C_2H_6 / Cl_2 mixture in presence of O_2. The reaction can proceed via a radical maintain channel leading to two C_2H_5O radicals (R1a) or to stable products (R1b/1c). Because C_2H_5O radicals react subsequently with O_2 leading to HO_2, which in term reacts rapidly with $C_2H_5O_2$, knowledge of the branching ratio is indispensable for retrieving the rate constant. A strong disagreement exists about the rate constant and the branching ratio between the IUPAC recommendation (Atkinson *et al*., ACP, 3525, 2006) and a recent, more direct measurement (Noell *et al*., JPC A, 6983, 2010). The rate constant for the self-reaction has been found at $k_1 = (1.0\pm0.2) \times 10^{-13}\ cm^3s^{-1}$ with the branching fraction of the C_2H_5O radical channel being $\alpha = (0.31\pm0.06)$, being in contradiction with the IUPAC recommendation, but confirms the most recent measurement and indicates that the current recommendation for this reaction should be revised. The reaction of $C_2H_5O_2$ with the ethoxy radical (C_2H_5O) can also been involved in the reaction mechanism, and its rate constant is also extracted from modelling. It is found to be $k_9 = (7\pm1.5) \times 10^{-12}\ cm^3s^{-1}$, two times slower than the only available measurement from Noell *et al*. JPC A, 6983, 2010.

INTRODUCTION

The oxidation of volatile organic compounds (VOCs) in the troposphere is mainly driven by hydroxyl radicals (OH) and leads, after addition of O_2, to the formation of organic peroxy radicals (RO_2). The fate of these RO_2 radicals depends on the chemical composition of the environment. In polluted atmospheres they mainly react with nitric oxide (NO) to form alkoxy radicals or react with nitrogen dioxide (NO_2) to form peroxynitrates (RO_2NO_2). Subsequent to the reaction with NO, alkoxy radicals react with O_2 to form hydroperoxy radicals (HO_2). HO_2 further oxidises NO into NO_2 and thus regenerates OH, closing the quasi-catalytic cycle. The photolysis of the produced NO_2 leads subsequently to the formation of ozone (O_3) and is the only relevant formation path of tropospheric ozone. In clean environments with low NO_x (NO_x = NO + NO_2)

concentrations, the fate of RO_2 change and their dominant loss becomes the reaction with HO_2 forming hydroperoxides ROOH and terminating the radical reaction chain. Other reaction pathways under low NOx conditions for RO_2 radicals are either reaction with other RO_2 as self- ($RO_2 + RO_2$) or cross-reaction ($RO_2 + R'O_2$) or with OH radicals ($RO_2 + OH$) [1-3].

Ethane is one of the most abundant non-methane hydrocarbons, and its atmospheric oxidation leads to the formation of the ethyl peroxy radical, $C_2H_5O_2$. Under low NO_x conditions the following reactions can occur for $C_2H_5O_2$:

- its self-reaction[4-14]

$$2\ C_2H_5O_2 \rightarrow 2\ C_2H_5O + O_2 \quad \text{(R1a)}$$

$$\rightarrow C_2H_5OH + CH_3CHO + O_2 \quad \text{(R1b)}$$

$$\rightarrow C_2H_5O_2C_2H_5 + O_2 \quad \text{(R1c)}$$

- its reaction with HO_2[4-5, 11, 15-18]

$$C_2H_5O_2 + HO_2 \rightarrow C_2H_5OOH + O_2 \quad \text{(R2)}$$

- its cross-reaction with other peroxy radicals, mainly CH_3O_2[19]

$$C_2H_5O_2 + CH_3O_2 \rightarrow 2\ C_2H_5O + CH_3O + O_2 \quad \text{(R3a)}$$

$$\rightarrow C_2H_5OH/CH_3OH + CH_3CHO/CH_2O + O_2 \quad \text{(R3b)}$$

$$\rightarrow C_2H_5O_2CH_3 + O_2 \quad \text{(R3c)}$$

- its reaction with OH radicals[20-21]

$$C_2H_5O_2 + OH \rightarrow C_2H_5O + HO_2 \quad \text{(R4a)}$$

$$\rightarrow C_2H_5OOOH \quad \text{(R4b)}$$

While (R2) has only one reaction path, the self- and cross reactions with other peroxy radicals can either lead to stable products (R1b and R1c, whereby R1c is thought to be minor) or maintain the radical pool (R1a). A reliable determination of the branching fraction is therefore important. However, the investigation of such reactions is not straight forward, because secondary chemistry cannot be avoided: the C_2H_5O product of the $C_2H_5O_2$ self-reaction (R1a) leads to formation of the HO_2 radicals, after rapid reaction with O_2

$$C_2H_5O + O_2 \rightarrow CH_3CHO + HO_2 \quad \text{(R5)}$$

whereby the HO_2 radicals will subsequently react with $C_2H_5O_2$ (R2). The rate constant of (R2) is faster than the rate constant of (R1), and thus the $C_2H_5O_2$ decay is accelerated by (R2). Therefore, determining the rate constant k_1 from observed $C_2H_5O_2$ decays depends on the branching ratio $\alpha = k_{1a} / k_1$ used in the data treatment: for a given experimental $C_2H_5O_2$ decay the retrieved rate

constant k_1 will decrease with increasing branching ratio.

Earlier studies of peroxy chemistry have either used time resolved UV absorption spectroscopy for the determination of the overall rate constant[4-12] or, for the determination of the branching ratio, end-product studies by FTIR[13-14] or by gas chromatography[7]. Direct observations of the HO_2 yield and thus measurement of the branching ratio is not possible in UV absorption studies because the steady-state HO_2 concentration, that builds-up from the (R1a) / (R5) reaction sequence, is rather low due to the fast consumption of HO_2 through (R2). So, even if a relative selectivity between $C_2H_5O_2$ and HO_2 can principally be obtained by UV absorption spectroscopy (the absorption cross section at 250 nm is ~8 times higher for $C_2H_5O_2$ than for HO_2, at 210 nm the ratio is ~2 in favour of HO_2), "clean" $C_2H_5O_2$ decays can be observed when studying (R1), however the corresponding HO_2 profiles cannot be extracted, because even at short wavelengths the much higher $C_2H_5O_2$ concentration compared to HO_2 always makes up the major fraction of the absorption signal, and a correction of the HO_2 profile for contribution of $C_2H_5O_2$ would induce very large error bars. Therefore, time-resolved UV absorption studies used the branching ratio, obtained from end-product studies, to extract the rate constant from the measured $C_2H_5O_2$ decays. This way, UV absorption measurements came to a relatively good agreement for the absolute value of the overall rate constant and end-product studies also came to a fairly good agreement on the branching ratio. Thus, it was agreed in almost all studies that the radical channel (R1a) is the major path, and a branching fraction of $\alpha = 0.63$ for (R1a) and a total rate constant of $k_1 = 7.6\times10^{-14}$ cm^3s^{-1} is currently recommended by the IUPAC committee[22].

More recently, Noell *et al.*[5] have carried out in 2010 for the first time a more selective measurement of this reaction: UV absorption was still used to monitor $C_2H_5O_2$, but HO_2 was directly measured in a selective way using wavelength modulation spectroscopy in the near IR. Interestingly, this work is in large disagreement with the earlier recommendations: while the observed $C_2H_5O_2$ decays were in agreement with the older data, a branching fraction of only $\alpha = 0.28$ was found for the radical path. This leads to an overall rate constant of $k_1 = 1.19\times10^{-13}$ cm^3s^{-1}, around 56% higher than the value currently recommended by IUPAC.

To our knowledge, no new measurements have been carried out on the $C_2H_5O_2$ self-reaction since this interesting finding of the important disagreement between the recommended IUPAC values and the results from Noell *et al*. It seems therefore important to reinvestigate this reaction with yet another selective detection method. Here, we present results of experiments that have been carried out using laser photolysis coupled to cw-CRDS absorption spectroscopy in the near

infrared region for a selective and sensitive detection of both radicals: the $C_2H_5O_2$ radical is quantified in the Ã-X̃ electronic transition at 7596.47 cm^{-1} (1316.4 nm), and the HO_2 radical is followed in the $2\nu_1$ overtone vibration band at 6638.2 cm^{-1} (1506.4 nm).

EXPERIMENTAL

Experimental setup

The setup has been described in detail before [23-26] and is only briefly discussed here (**Figure 1)**.

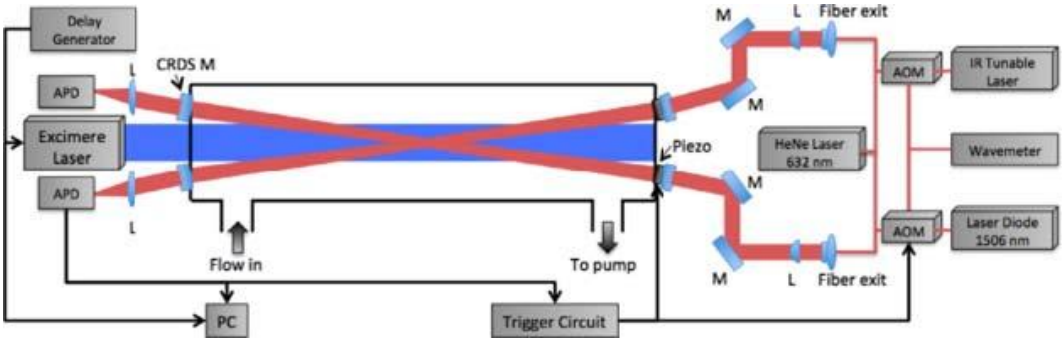

Figure 1. Schematic view of the experimental setup: AOM, Acousto-Optic Modulator; APD, Avalanche Photo Diode; M, Mirror; L, Lens. Both cw-CRDS systems are equipped with identical trigger circuits and data acquisition systems.

The setup consisted of a 0.79 m long flow reactor made of stainless steel. The beam of a pulsed excimer laser (Lambda Physik LPX 202i, XeF at 351 nm) passed the reactor longitudinally. The flow reactor contained two identical continuous wave cavity ring-down spectroscopy (cw-CRDS) absorption paths, which were installed in a small angle with respect to the photolysis path. An overlap with the photolysis beam of 0.28 m is achieved with an excimer beam width delimited to 2 cm. Both beam paths were tested for a uniform overlap with the photolysis beam before experiments were done. For this purpose, both cw-CRDS instruments were operated to simultaneously measure HO_2 concentrations. Deviations between HO_2 concentrations were less than 5 % demonstrating that the photolysis laser was very well aligned, *i.e.* both light paths probed a very similar photolysed volume in the reactor. A small helium purge flow prevented the mirrors from being contaminated. Two different DFB lasers are used for the detection of the two species ($C_2H_5O_2$, HO_2). They are coupled into one of the cavities by systems of lenses and

mirrors. Each probe beam passed an acousto-optic modulator (AOM, AAoptoelectronic) to rapidly turn off the 1st order beam once a threshold for light intensity in the cavity was reached, in order to measure the ring-down event. Then, the decay of light intensity was recorded and an exponential fit is applied to retrieve the ring-down time. The absorption coefficient α is derived from Equation (1).

$$\alpha = [A] * \sigma_A = \frac{R_L}{c}\left(\frac{1}{\tau} - \frac{1}{\tau_0}\right) \quad \text{(Eq. 1)}$$

where τ is the ring-down time with an absorber present; τ_0 is the ring-down time with no absorber present; σ_A is the absorption cross section of the absorbing species A; R_L is the ratio between cavity length (79 cm) and effective absorption path (28.8 cm); c is the speed of light.

Ethylperoxy radicals were generated by pulsed 351 nm photolysis of C_2H_6 / Cl_2 / O_2 mixtures:

$$Cl_2 + h\nu_{351\ nm} \rightarrow 2\ Cl \quad \text{(R6)}$$

$$C_2H_6 + Cl \rightarrow C_2H_5 + HCl \quad \text{(R7)}$$

$$C_2H_5 + O_2 + M \rightarrow C_2H_5O_2 + M \quad \text{(R8a)}$$

$$C_2H_5 + O_2 \rightarrow C_2H_4 + HO_2 \quad \text{(R8b)}$$

In order to rapidly convert C_2H_5O into HO_2 through reaction (R5), most experiments have been carried out in 100 Torr O_2 (Air Liquide, Alphagaz 2). In order to investigate the possible secondary reaction

$$C_2H_5O_2 + C_2H_5O \rightarrow \text{products} \quad \text{(R9)}$$

some experiments have been carried out in 90 Torr N_2 / 10 Torr O_2.

Ethane (Mitry-Mory, N35) was used directly from the cylinder: a small flow was added to the mixture through a calibrated flow meter (Bronkhorst, Tylan). All experiments were carried out at 298 K.

RESULTS AND DISCUSSION

The reliability of the measurement depends on the selective and sensitive detection of HO_2 and $C_2H_5O_2$ radicals: these two aspects will be presented at first. When studying the self-reaction of $C_2H_5O_2$, several secondary reactions can be important and will need to be taken into account: the reaction of $C_2H_5O_2$ with HO_2 (R2) and with C_2H_5O (R9). Because data for these reactions are

sparse, we have studied them separately and the results will be presented individually thereafter.

Detection of HO_2 radicals

The reliability of the measurements presented in this work depends on the selective quantification of the two radicals, HO_2 and $C_2H_5O_2$. HO_2 has been detected on the strongest line of the $2\nu_1$ band at 6638.2 cm^{-1}. Pressure dependent absorption cross sections in helium ($\sigma_{50\ Torr\ He} = 2.72\times10^{-19}$ cm^2) [27-28] and in synthetic air[29-31] ($\sigma_{100\ Torr\ air} = 1.44\times10^{-19}$ cm^2) have been measured several times, but the cross section in pure O_2 had only been measured once for a rather small absorption line[32]. Recently, we have determined the absorption cross section for the strong line at 6638.2 cm^{-1} at 100 Torr O_2[33], and the value of $\sigma_{100\ Torr\ O2} = 2.0\times10^{-19}$ cm^2 is used in this work to convert absorption-time profiles of HO_2 into concentration time profiles. The absorption spectrum of HO_2 in this wavelength range is very structured with sharp peaks, thus it is easy to verify the selectivity of the measurement towards HO_2 by taking absorption measurements on top of the line, and at a wavelength just next to it, where the HO_2 absorption is virtually zero. No absorption signal was observed off the HO_2 line in any of the current experiments, and therefore we can conclude that absorption measurements at 6638.2 cm^{-1} are highly selective for HO_2 radicals in this reaction system.

Detection of $C_2H_5O_2$ radicals

The detection of $C_2H_5O_2$ in the near IR is less clear-cut: there was neither good agreement on the absorption cross section[34-36] nor is the spectrum as structured as HO_2, which makes it less straightforward to verify the selectivity of the measurement. Recently, we have determined the absorption cross section of $C_2H_5O_2$ in $\tilde{A}$-$\tilde{X}$ electronic transition[33] and have obtained a pressure independent absorption cross section of $\sigma = 1.0\times10^{-20}$ cm^2 on the peak at 7596.47 cm^{-1}. This cross section is used in the current work to convert $C_2H_5O_2$ absorption time profiles into concentration time profiles.

To assure that the decays measured at the peak wavelength of $C_2H_5O_2$ are selective for this radical, it is not possible to measure, as for HO_2, decays at a wavelength where $C_2H_5O_2$ does not absorb, as the transition is too broad. Therefore, kinetic decays have been measured at several different wavelengths that are accessible with our DFB laser: in the case of an underlying absorption of another species, for example a reaction product, one can expect that the shape of the absorption spectrum for any other species would be different from the shape of the spectrum

of $C_2H_5O_2$. Indeed, it has been shown[33] that the absorption cross section of $C_2H_5O_2$ varies over a factor of 5 in the range between 7596 and 7630 cm^{-1} and an underlaying absorption of another species with a less or differently varying spectrum should lead to different shapes of kinetic decays at different wavelengths: the influence of the co-absorbing species on the shape of the decay should be highest at wavelengths where the $C_2H_5O_2$ absorption is lowest. In **Figure 2** are shown examples of five decays measured at wavelengths between the peak (open red dots) and the wavelength with the lowest $C_2H_5O_2$ cross section (black dots), all obtained under the same conditions following the 351 nm photolysis of Cl_2 / C_2H_6 mixtures. A very high initial radical concentration has deliberately been used to force formation of high concentrations of reaction products. Even under these conditions no change in the shape of the decays can be observed for the different wavelengths, and therefore we conclude that measurements at 7596.47 cm^{-1} are selective measurements of $C_2H_5O_2$ in this reaction system.

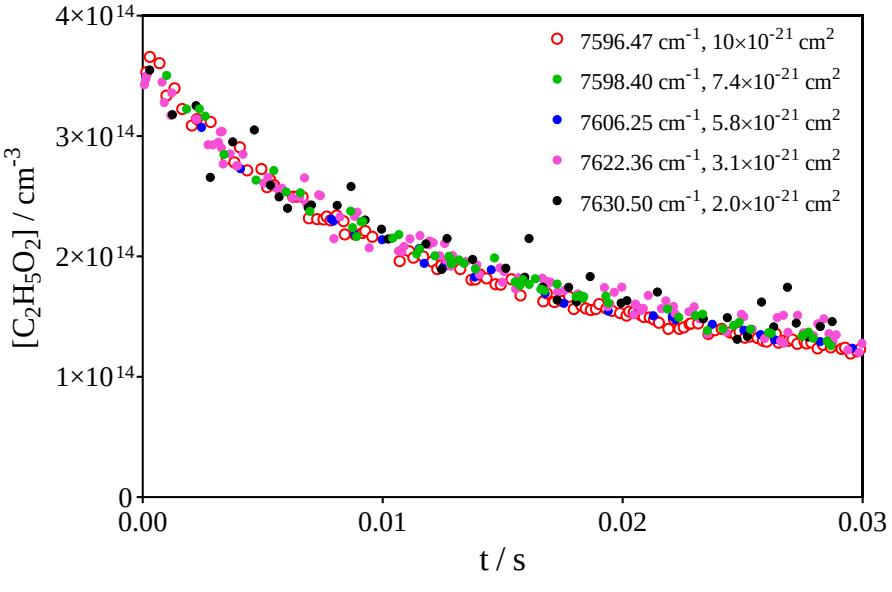

Figure 2: Examples of $C_2H_5O_2$ decays following the 351 nm photolysis $[Cl_2] = 3\times10^{16}$ cm^{-3} in presence of $[C_2H_6] = 2.6\times10^{16}$ cm^{-3}, obtained at 5 different wavelengths: the absorption cross section of $C_2H_5O_2$ (given in the legend of the figure) varies over a factor of 5 for the different wavelengths

Rate constant of the reaction of $C_2H_5O_2$ with HO_2

As explained in the introduction, the reaction of HO_2 with $C_2H_5O_2$ (R2) plays a major role during the self-reaction of $C_2H_5O_2$ and knowing its rate constant is therefore essential for extracting the branching ratio of (R1). Despite several measurements[4-5, 11, 15-18], there was no good agreement

for this rate constant, and even the two most recent and considered being the most reliable determinations varied by about a factor of 1.5 (8.14×10^{-12} $cm^{-3}s^{-1}$ for Boyd *et al.*[17] from UV absorption and 5.57×10^{-12} $cm^{-3}s^{-1}$ for Noell *et al.*[5] from UV / near IR absorption), with the IUPAC recommended value being the average of both rate constants (6.9×10^{-12} $cm^{-3}s^{-1}$). For this reason, we have recently determined this rate constant again[33], and have found with $k_2 = 6.2\times10^{-12}$ $cm^{-3}s^{-1}$ a rate constant that rather confirms the lower value such as obtained by Noell *et al*. This rate constant is used in this work for the evaluation of the experimental data on the self-reaction of $C_2H_5O_2$.

Rate constant of the reaction of $C_2H_5O_2$ with C_2H_5O

In the work of Noell *et al.*[5] it turned out, that the reaction of $C_2H_5O_2$ with C_2H_5O (R9) played some role under their conditions, and in experiments using different O_2 concentrations they extracted a fast rate constant of $k_9 = 1.5\times10^{-11}$ $cm^{-3}s^{-1}$ for this reaction. Even though experiments in this work were carried out in 100 Torr O_2 (compared to 50 Torr O_2 in Noell *et al*.) making (R5) very rapid ($k_5' \approx 24.000$ s^{-1}) and thus the stationary concentration of C_2H_5O very low, it turned out during data evaluation of the self-reaction experiments, that (R9) would still have a small impact on the HO_2 profiles (decreasing HO_2 with increasing initial radical concentration) when using the fast rate constant from Noell *et al*.[5] For this reason, we have carried out some experiments with low O_2 concentration in order to re-determine k_9 under our conditions. In **Figure 3** are shown experiments using 4 different initial Cl-concentrations: in the left graph are shown experiments carried out under low O_2 (90 Torr N_2 and 10 Torr O_2: $[O_2] \sim 3\times10^{17}$ cm^{-3}), experiments in the right graph were carried out under high O_2 (100 Torr O_2: $[O_2] \sim 3\times10^{18}$ cm^{-3}). It can be seen that the $C_2H_5O_2$ profiles (lower graphs) are very similar between the two conditions, however the HO_2 profiles (upper graphs) present strong differences:

- the HO_2 concentrations just after the photolysis pulse are higher in the case of 100 Torr O_2 compared to 90 Torr N_2 / 10 Torr O_2. This is in line with the hypotheses that this initial HO_2 is formed in collision between hot C_2H_5 and O_2: with increasing N_2 and decreasing O_2, collisions with N_2 will cool down excited C_2H_5 and (R8b) will get less important.
- HO_2 signals initially rise in the case of high O_2 while they decay from the beginning in the case of low O_2. At high O_2, HO_2 formation from the reaction sequence (R1 / R5) is initially faster (due to the fast conversion of C_2H_5O ($k_5' = 24.000$ s^{-1})) than its consumption through (R2), until after 2-3 ms steady-state is reached and HO_2 decays at

the same pace as $C_2H_5O_2$. Under low O_2, conversion of C_2H_5O into HO_2 (R5) is 10 times slower and the reaction with $C_2H_5O_2$ becomes competitive for C_2H_5O, the formation of HO_2 through the reaction sequence (R1 / R5) is slower than (R2).

An initial model using the rate constant for (R9) such as recommended by Noell *et al.* (k_9 = 1.5×10^{-11} $cm^{-3}s^{-1}$) did not allow to reproduce the HO_2 profiles under low O_2 condition: using this rate constant, the modelled HO_2 profiles decreased much faster than the experimental profiles (dashed lines in the upper graph of **Figure 3**). The HO_2 profiles were best reproduced when using a rate constant of k_9 = 7×10^{-12} $cm^{-3}s^{-1}$, nearly 2 times slower (full lines in the upper graphs of **Figure 3**). The rising profiles in the upper graphs of **Figure 3** show the product of the reaction of $C_2H_5O_2$ + C_2H_5O: the right y-axis applies, and it should be noted that the axis ends at 3×10^{13} cm^{-3}, to be compared with the left scale for the HO_2 profile which ends at 2×10^{12} cm^{-3}. It can be seen that even with the lower rate constant, this reaction plays some role, especially under low O_2 conditions. Ignoring this reaction does not allow reproducing our HO_2 profiles under low O_2 neither: the modelled profile without (R9) is shown as the dashed-dotted line, only for the highest radical concentration.

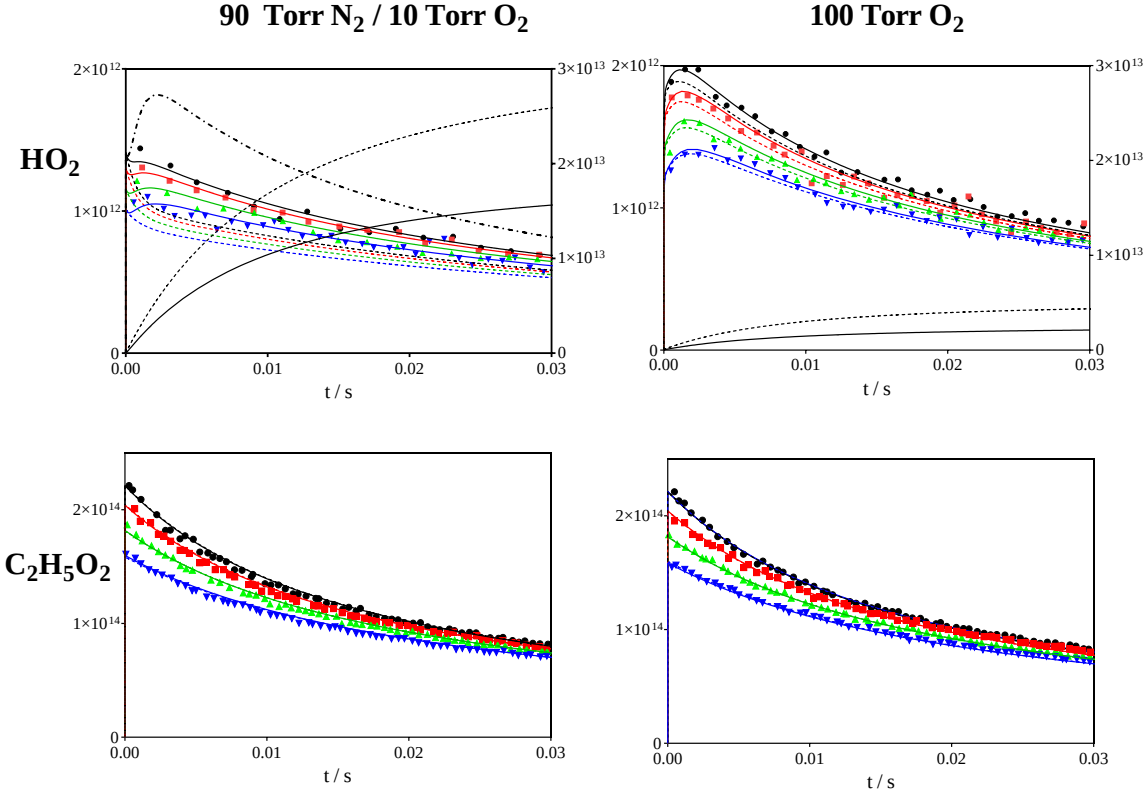

Figure 3: Experiments for determination of the rate constant between $C_2H_5O_2$ and C_2H_5O: upper graphs show HO_2 profiles, lower graphs show simultaneously measured $C_2H_5O_2$ profiles. Left graphs: 90 Torr N_2 / 10 Torr O_2, right graphs: 100 Torr O_2. Initial Cl-concentration was 2.26,

2.08, 1.85 and 1.6×10^{14} cm^{-3} for the experiments marked with black, red, green and blue dots, respectively. Full lines: model with k_9 = 7×10^{-12} cm^{3}s^{-1}, dotted coloured lines k_9 = 1.5×10^{-11} cm^{3}s^{-1}, dashed-dotted black line k_9 = 0, for highest radical concentration only. Rising profiles in the upper graph show the product of (R9: $C_2H_5O_2$ + C_2H_5O) right y-axis applies.

Not many detail are given in the earlier work of Noell *et al.* on how the rate constant was determined, therefore it is difficult to understand the differences and no good explanation can be given for the disagreement of our results with the result from Noell *et al.*[5]. From these experiments we have chosen to use k_9 = 7×10^{-12} cm^{-3}s^{-1} for the evaluation of the $C_2H_5O_2$ self-reaction experiments. It should however be noted that this reaction has a smaller impact on the retrieved rate constant and branching ratio of the self-reaction experiments due to the 2 times higher O_2 concentration used in our experiments, compared to Noell *et al.*

Rate constant and branching ratio of the self-reaction of $C_2H_5O_2$

The rate constant of the self-reaction of $C_2H_5O_2$ has been measured in this work by following simultaneously $C_2H_5O_2$ and HO_2. **Figure 4** shows an example of profiles obtained from the photolysis of varying concentrations of Cl_2 in presence of [C_2H_6] = 2×10^{16} cm^{-3} and [O_2] = 3×10^{18} cm^{-3}. The HO_2 profiles do not start at zero just after the laser pulse: this is due to (R8b), leading to the formation of around 1% or less of HO_2 next to the major product $C_2H_5O_2$ in the reaction of C_2H_5 + O_2. This has already been observed in earlier works[5, 37].

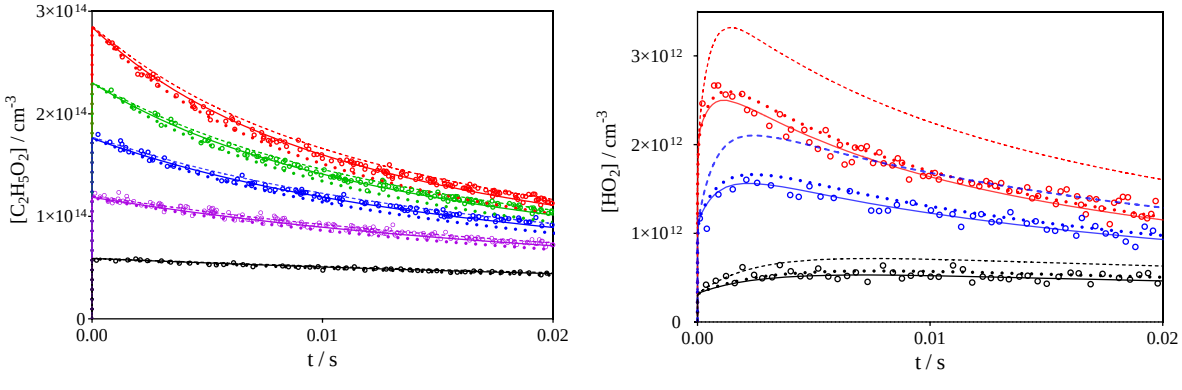

Figure 4: $C_2H_5O_2$ (left graph) and HO_2 (right graph) profiles obtained from the 351 nm photolysis of [Cl_2] = 0.6, 1.3, 1.9, 2.5, and 3 ×10^{16} cm^{-3}, from bottom to top (for clarity, green and purple HO_2 data are not shown). Full lines model from **Table 1,** dotted lines model using values from Noell *et al.*, dashed lines model with IUPAC recommended values for k_{1a} and k_{1b} (see **Table 2**).

High C_2H_6 concentrations (2-3×10^{16} cm^{-3}) have always been used in order to minimize the impact of the fast reaction of Cl-atoms with $C_2H_5O_2$. Also, most experiments have been carried out at 100 Torr O_2 in order to make (R5) as fast as possible and minimize the impact of (R9) (see above paragraph). The rate constant k_1 and the branching fraction α have then been extracted by fitting both HO_2 and $C_2H_5O_2$ profiles simultaneously for an entire series of experiments with varying Cl-concentrations. In the example in **Figure 4**, the initial radical concentration has been changed by around a factor of 6, making the reactivity of $C_2H_5O_2$ varying on our typical time scale of 20 ms from near stable for the lowest concentration (black symbols) to a loss of more than 50% of $C_2H_5O_2$ for the highest concentration (red symbols). The loss due to diffusion is nearly negligible in this time window as can be seen from the black line. The rate constant k_{8b}, *i.e.* the fraction of C_2H_5 radicals that leads in the reaction with O_2 to direct formation of HO_2 radicals, has been adjusted such as to best reproduce the non-zero HO_2 concentration immediately after the photolysis pulse. This fraction was always around 1%, in good agreement with earlier findings.

Table 1: Reaction mechanism used to fit all experiments in this work

	Reaction	**k / cm^3s^{-1}**	**Reference**
1a	2 $C_2H_5O_2$ → 2 C_2H_5O + O_2	3.2 × 10^{-14}	This work
1b	2 $C_2H_5O_2$ → C_2H_5OH + CH_3CHO + O_2	7.0 × 10^{-14}	This work
2	$C_2H_5O_2$ + HO_2 → C_2H_5OOH + O_2	6.2 × 10^{-12}	Ref[33]
5	C_2H_5O + O_2 → CH_3CHO + HO_2	8 × 10^{-15}	Ref[38]
7	Cl + C_2H_6 → C_2H_5 + HCl	5.9 × 10^{-11}	Ref[22]
8a	C_2H_5 + O_2 + M → $C_2H_5O_2$ + M	4.8 × 10^{-12}	Ref[39]
8b	C_2H_5 + O_2 → C_2H_4 + HO_2	3-4× 10^{-14}	This work
9	$C_2H_5O_2$ + C_2H_5O → products	7 × 10^{-12}	This work
10	2 HO_2 → H_2O_2 + O_2	1.7 × 10^{-12}	Ref [40]
11	C_2H_5O + HO_2 → products	1 × 10^{-10}	Ref [41]
12	$C_2H_5O_2$ → diffusion	2 s^{-1}	This work
13	HO_2 → diffusion	3 s^{-1}	This work

The full lines in **Figure 4** show the result of the model such as given in **Table 1**. Both radical profiles are very well reproduced over the full range of initial radical concentrations. **Figure 4** also includes the results of two other models with the rate constants of (R1), (R2) and (R9) varied to match either the results from Noell *et al.*[5], (dotted lines) or the current IUPAC

recommendations[22] (dashed lines): the rate constants used for these models are summarized in **Table 2**.

Table 2: Values used for models in **Figure 4**, all rate constants are in units $cm^3\ s^{-1}$.

	Reaction	This work	Noell *et al.* [5]	IUPAC[22]
1a	$2\ C_2H_5O_2 \rightarrow 2\ C_2H_5O + O_2$	3.2×10^{-14}	3.33×10^{-14}	4.79×10^{-14}
1b	$2\ C_2H_5O_2 \rightarrow C_2H_5OH + CH_3CHO + O_2$	7.0×10^{-14}	8.57×10^{-14}	2.81×10^{-14}
1	$k / 10^{-13}\ cm^3 s^{-1}$	1.0±0.2*	1.19±0.04	0.76±0.4
1	$k_{obs} / 10^{-13}\ cm^3 s^{-1}$	1.34	1.52	1.24
1	α	0.31±0.06*	0.28±0.06	0.63
2	$C_2H_5O_2 + HO_2 \rightarrow C_2H_5OOH + O_2$	$(6.2\pm1.5)\times10^{-12}$	$(5.6\pm0.4)\times10^{-12}$	6.9×10^{-12}
10	$C_2H_5O_2 + C_2H_5O \rightarrow$ products	$(7\pm1.5)^* \times 10^{-12}$	$(15\pm7) \times 10^{-12}$	-

*Error bars of 20% are estimated, mostly due to uncertainties in the absolute absorption cross sections of HO_2 and $C_2H_5O_2$

Using the IUPAC recommended values[22], the deviation of the model from our $C_2H_5O_2$ measurements is very minor (the model decays too slowly), however the disagreement of the model with our HO_2 profiles is huge: the model predicts too much HO_2, far beyond any experimental uncertainty. This is due to the much higher radical yield in (R1), which is not counterbalanced by the overall slower rate constant k_1 or the faster rate constant of (R2). The agreement with the model using the rate constants from Noell *et al.* [5] is very good for the HO_2 profiles (the model slightly overpredicts the HO_2 concentration by around 10%, within the experimental uncertainty) , but for $C_2H_5O_2$ the model predicts too fast decays, especially at longer reaction times. This slight disagreement is due to a combination of different rate constants used in both models for the three major radical-radical reactions: the higher rate constant of (R9), a lower rate constant of (R2) and a slightly faster (R1) with a lower radical yield from the work of Noell *et al*. Again, this slight disagreement is within the experimental uncertainty, especially given that several radical-radical reactions are involved, and therefore, even though the agreement of our measurements with the data from Noell *et al*.[5] is not perfect, it confirms their finding of an overall faster rate constant for (R1) together with a lower branching ratio for the radical channel, compared to current recommendations.

An extensive discussion on the comparison with earlier determination of the rate constant and

branching ratio for (R1), together with possible reasons for the important disagreement for the branching ratio, obtained by either end-product analysis or by direct detection of HO_2, has been given by Noell *et al*. and will not be repeated here.

CONCLUSION

The rate constant and branching ratio of the self-reaction of $C_2H_5O_2$ radicals has been measured using a selective cw-CRDS detection of HO_2 and $C_2H_5O_2$ in the $\tilde{A}$-$\tilde{X}$ electronic transition located in the near-IR region. Large discrepancy existed for the rate constant and branching ratio of this reaction: a high C_2H_5O radical yield was generally admitted, based on stable end product measurements of experiments carried out in the 1990's[4-14], while a more recent work using selective detection of HO_2 radicals found the radical channel to be the minor one[5]. In this work we have also directly measured the radical yield and confirmed that it should take a low value (α = 0.31±0.06), together with a faster overall rate constant (k_1 = (1.0±0.2) × 10^{-13} cm^3 s^{-1}). This is therefore the second report of a low radical yield, based on direct measurement of radicals rather than end-products. Therefore, it is proposed that the IUPAC committee should revise their recommendation and that these lower branching fraction and faster rate constant are implemented in atmospheric chemical models. Because the reaction of $C_2H_5O_2$ with the alkoxy radical C_2H_5O plays some role under our experimental conditions, presently its rate constant has also been measured and found to be k_9 = (7±1.5) × 10^{-12} cm^3 s^{-1}.

ACKNOWLEDGEMENT

This project was supported by the French ANR agency under contract No. ANR-11-Labx-0005-01 CaPPA (Chemical and Physical Properties of the Atmosphere), the Région Hauts-de-France, the Ministère de l'Enseignement Supérieur et de la Recherche (CPER Climibio) and the European Fund for Regional Economic Development. X.T. would like to thank the National Natural Science Foundation of China (No. 21773249) and C.Z. thanks the Chinese Scholarship Council for financial support (No. 202006340125).

REFERENCES

1. Orlando, J. J.; Tyndall, G. S., Laboratory studies of organic peroxy radical chemistry: an overview with emphasis on recent issues of atmospheric significance. *Chem. Soc. Rev.* **2012**, *41*, 6294-317.
2. Fittschen, C., The reaction of peroxy radicals with OH radicals. *Chem. Phys. Lett.* **2019**, *725*, 102-108.
3. Assaf, E.; Song, B.; Tomas, A.; Schoemaecker, C.; Fittschen, C., Rate Constant of the Reaction between CH_3O_2 Radicals and OH Radicals revisited. *J. Phys. Chem. A* **2016**, *120*, 8923-8932.
4. Cattell, F. C.; Cavanagh, J.; Cox, R. A.; Jenkin, M. E., A kinetic study of reactions of HO_2 and $C_2H_5O_2$ using diode-laser absorption spectroscopy. *Journal of the Chemical Society-Faraday Transactions Ii* **1986**, *82*, 1999-2018.
5. Noell, A. C.; Alconcel, L. S.; Robichaud, D. J.; Okumura, M.; Sander, S. P., Near-Infrared Kinetic Spectroscopy of the HO_2 and $C_2H_5O_2$ Self-Reactions and Cross Reactions. *J. Phys. Chem. A* **2010**, *114*, 6983-6995.
6. Adachi, H.; Basco, N.; James, D. G. L., Ethylperoxy Radical Spectrum and Rate Constant for mutual Interaction measured by Flash-Photolysis and Kinetic Spectroscopy. *Int. J. Chem. Kinet.* **1979**, *11*, 1211-1229.
7. Anastasi, C.; Waddington, D. J.; Woolley, A., Reactions of Oxygenated Radicals in the Gas-Phase. 10. Self-Reactions of Ethylperoxy Radicals. *Journal of the Chemical Society-Faraday Transactions I* **1983**, *79*, 505-516.
8. Munk, J.; Pagsberg, P.; Ratajczak, E.; Sillesen, A., Spectrokinetic Studies of Ethyl and Ethylperoxy Radicals. *J. Phys. Chem.* **1986**, *90*, 2752-2757.
9. Wallington, T. J.; Dagaut, P.; Kurylo, M. J., Measurements of the Gas-Phase UV Absorption-Spectrum of $C_2H_5O_2$. Radicals and the Temperature-Dependence of the Rate-Constant for their Self-Reaction. *Journal of Photochemistry and Photobiology a-Chemistry* **1988**, *42*, 173-185.
10. Bauer, D.; Crowley, J. N.; Moortgat, G. K., The UV absorption spectrum of the ethylperoxy radical and its self-reaction kinetics between 218 and 333 K. *J. Photochem. Photobiol. A* **1992**, *65*, 329-344.
11. Fenter, F. F.; Catoire, V.; Lesclaux, R.; Lightfoot, P. D., The ethylperoxy radical: its ultraviolet spectrum, self-reaction, and reaction with hydroperoxy, each studied as a function of temperature. *J. Phys. Chem.* **1993**, *97*, 3530-3538.
12. Atkinson, D. B.; Hudgens, J. W., Chemical Kinetic Studies Using Ultraviolet Cavity Ring-Down Spectroscopic Detection: Self-Reaction of Ethyl and Ethylperoxy Radicals and the Reaction $O_2 + C_2H_5 \rightarrow C_2H_5O_2$. *J. Phys. Chem. A* **1997**, *101*, 3901-3909.
13. Niki, H.; Maker, P. D.; Savage, C. M.; Breitenbach, L. P., Fourier-Transform Infrared Studies of the Self-Reaction of $C_2H_5O_2$ Radicals. *J. Phys. Chem.* **1982**, *86*, 3825-3829.
14. Wallington, T. J.; Gierczak, C. A.; Ball, J. C.; Japar, S. M., Fourier-Transform Infrared Study of the Self-Reaction of $C_2H_5O_2$ Radicals in Air at 295 K. *Int. J. Chem. Kinet.* **1989**, *21*, 1077-1089.
15. Dagaut, P.; Wallington, T. J.; Kurylo, M. J., Flash photolysis kinetic absorption spectroscopy study of the gasphase reaction $HO_2 + C_2H_5O_2$ over the temperature range 228 - 380K. *J. Phys. Chem.* **1988**, *92*, 3836-3839.
16. Maricq, M. M.; Szente, J. J., A Kinetic Study of the Reaction between Ethylperoxy

Radicals and HO_2. *J. Phys. Chem.* **1994**, *98*, 2078-2082.
17. Boyd, A. A.; Flaud, P.-M.; Daugey, N.; Lesclaux, R., Rate Constants for RO_2 + HO_2 Reactions Measured under a Large Excess of HO_2. *J. Phys. Chem. A* **2003**, *107*, 818-821.
18. Raventós-Duran, M. T.; Percival, C. J.; McGillen, M. R.; Hamer, P. D.; Shallcross, D. E., Kinetics and branching ratio studies of the reaction of $C_2H_5O_2$ + HO_2 using chemical ionisation mass spectrometry. *Phys. Chem. Chem. Phys.* **2007**, *9*, 4338 - 4348.
19. Villenave, E.; Lesclaux, R., Kinetics of the Cross Reactions of CH_3O_2 and $C_2H_5O_2$ Radicals with Selected Peroxy Radicals. *J. Phys. Chem.* **1996**, *100*, 14372-14382.
20. Faragó, E. P.; Schoemaecker, C.; Viskolcz, B.; Fittschen, C., Experimental Determination of the Rate Constant of the Reaction between $C_2H_5O_2$ and OH Radicals. *Chem. Phys. Lett.* **2015**, *619*, 196-200.
21. Assaf, E.; Schoemaecker, C.; Vereecken, L.; Fittschen, C., Experimental and Theoretical Investigation of the Reaction of RO_2 Radicals with OH Radicals: Dependence of the HO_2 Yield on the Size of the Alkyl Group. *Int. J. Chem. Kinet.* **2018**, *50*, 670–680.
22. Atkinson, R.; Baulch, D. L.; Cox, R. A.; Crowley, J. N.; Hampson, R. F.; Hynes, R. G.; Jenkin, M. E.; M. J. Rossi; Troe, J., Evaluated Kinetic and Photochemical Data for Atmospheric Chemistry: Volume II - Gas Phase Reactions of Organic Species. *Atmos. Chem. Phys.* **2006**, *6*, 3625-4055.
23. Thiebaud, J.; Fittschen, C., Near Infrared cw-CRDS Coupled to Laser Photolysis: Spectroscopy and Kinetics of the HO_2 Radical. *Appl. Phys. B* **2006**, *85*, 383-389.
24. Parker, A. E.; Jain, C.; Schoemaecker, C.; Szriftgiser, P.; Votava, O.; Fittschen, C., Simultaneous, time-resolved measurements of OH and HO_2 radicals by coupling of high repetition rate LIF and cw-CRDS techniques to a laser photolysis reactor and its application to the photolysis of H_2O_2. *Appl. Phys. B.* **2011**, *103*, 725-733.
25. Votava, O.; Mašát, M.; Parker, A. E.; Jain, C.; Fittschen, C., Microcontroller based resonance tracking unit for time resolved continuous wave cavity-ringdown spectroscopy measurements. *Rev. Sci. Instrum.* **2012**, *83*, 043110.
26. Assaf, E.; Asvany, O.; Votava, O.; Batut, S.; Schoemaecker, C.; Fittschen, C., Measurement of line strengths in the $\tilde{A}\ ^2A' \leftarrow X\ ^2A''$ transition of HO_2 and DO_2. *J. Quant. Spectrosc. Radiat. Transfer* **2017**, *201*, 161-170.
27. Thiebaud, J.; Crunaire, S.; Fittschen, C., Measurement of Line Strengths in the $2\nu_1$ Band of the HO_2 Radical using Laser Photolysis / Continous wave Cavity Ring Down Spectroscopy (cw-CRDS). *J. Phys. Chem. A* **2007**, *111*, 6959-6966.
28. Tang, Y.; Tyndall, G. S.; Orlando, J. J., Spectroscopic and Kinetic Properties of HO_2 Radicals and the Enhancement of the HO_2 Self Reaction by CH_3OH and H_2O. *J. Phys. Chem. A* **2010**, *114*, 369-378.
29. Ibrahim, N.; Thiebaud, J.; Orphal, J.; Fittschen, C., Air-Broadening Coefficients of the HO_2 Radical in the $2v_1$ Band Measured Using cw-CRDS. *J. Mol. Spectrosc.* **2007**, *242*, 64-69.
30. Assaf, E.; Liu, L.; Schoemaecker, C.; Fittschen, C., Absorption spectrum and absorption cross sections of the $2v_1$ band of HO_2 between 20 and 760 Torr air in the range 6636 and 6639 cm^{-1}. *Journal of Quantitative Spectroscopy & Radiative Transfer* **2018**, *211*, 107-114.
31. Onel, L.; Brennan, A.; Gianella, M.; Ronnie, G.; Lawry Aguila, A.; Hancock, G.; Whalley, L.; Seakins, P. W.; Ritchie, G. A. D.; Heard, D. E., An intercomparison of HO2 measurements by fluorescence assay by gas expansion and cavity ring-down spectroscopy within HIRAC (Highly Instrumented Reactor for Atmospheric Chemistry). *Atmos. Meas. Tech.* **2017**, *10*, 4877-4894.

32. Assali, M.; Rakovsky, J.; Votava, O.; Fittschen, C., Experimental determination of the rate constants of the reactions of HO2 + DO2 and DO2 + DO2. *International Journal of Chemical Kinetics* **2020**, *52*, 197-206.

33. Zhang, C.; Shamas, M.; Assali, M.; Tang, X.; Zhang, W.; Pillier, L.; Schoemaecker, C.; Fittschen, C., Absolute Absorption Cross-Section of the $\tilde{A}\leftarrow\tilde{X}$ Electronic Transition of the Ethyl Peroxy Radical and Rate Constant of Its Cross Reaction with HO_2. *Photonics* **2021**, *8*, 296.

34. Atkinson, D. B.; Spillman, J. L., Alkyl Peroxy Radical Kinetics Measured Using Near-infrared CW-Cavity Ring-down Spectroscopy. *J. Phys. Chem. A* **2002**, *106*, 8891-8902.

35. Rupper, P.; Sharp, E. N.; Tarczay, G.; Miller, T. A., Investigation of Ethyl Peroxy Radical Conformers via Cavity Ringdown Spectroscopy of the Ã- X Electronic Transition. *J. Phys. Chem. A* **2007**, *111*, 832–840.

36. Melnik, D.; Chhantyal-Pun, R.; Miller, T. A., Measurements of the Absolute Absorption Cross Sections of the A-X Transition in Organic Peroxy Radicals by Dual-Wavelength Cavity Ring-Down Spectroscopy. *J. Phys. Chem. A* **2010**, *114*, 11583-11594.

37. Clifford, E. P.; Farrell, J. T.; DeSain, J. D.; Taatjes, C. A., Infrared Frequency-Modulation Probing of Product Formation in Alkyl + O2 Reactions: I. The Reaction of C2H5 with O2 between 295 and 698 K. *J. Phys. Chem. A* **2000**, *104*, 11549-11560.

38. Fittschen, C.; Frenzel, A.; Imrik, K.; Devolder, P., Rate Constants for the Reactions of C_2H_5O, i-C_3H_7O, and n-C_3H_7O with NO and O_2 as a Function of Temperature. *Int. J. Chem. Kinet.* **1999**, *31*, 860-866.

39. Fernandes, R. X.; Luther, K.; Marowsky, G.; Rissanen, M. P.; Timonen, R.; Troe, J., Experimental and Modeling Study of the Temperature and Pressure Dependence of the Reaction $C_2H_5 + O_2$ (+ M) $\rightarrow$ $C_2H_5O_2$ (+ M). *J. Phys. Chem. A* **2015**, *119*, 7263-7269.

40. Atkinson, R.; Baulch, D. L.; Cox, R. A.; Crowley, J. N.; Hampson, R. F.; Hynes, R. G.; Jenkin, M. E.; Rossi, M. J.; Troe, J., Evaluated Kinetic and Photochemical Data for Atmospheric Chemistry: Volume 1 – Gas Phase Reactions of O_x, HO_x, NO_x, and SO_x, Species. *Atmos. Chem. Phys.* **2004**, *4*, 1461-1738.

41. Assaf, E.; Schoemaecker, C.; Vereecken, L.; Fittschen, C., The reaction of fluorine atoms with methanol: yield of CH_3O/CH_2OH and rate constant of the reactions $CH_3O + CH_3O$ and $CH_3O + HO_2$. *Phys. Chem. Chem. Phys.* **2018**, *20*, 8707.